1998 J.C. Polanyi Award Lecture Fullerene ions in the gas phase: chemistry as a function of charge state[1]

Diethard K. Böhme

Abstract: Results of recent measurements in the Ion Chemistry Laboratory at York University using the Selected-Ion Flow Tube (SIFT) technique are surveyed for reactions of singly, doubly, and triply charged buckminsterfullerene C_{60}^{n+} cations proceeding at room temperature in helium buffer gas at 0.35 Torr (1 Torr = 133.3 Pa). Measured rate coefficients and observed product channels for reactions with a variety of inorganic and organic molecules depend strongly on the charge state of the reactant ion. The measured rate coefficients span more than four orders of magnitude. Primary product channels observed include attachment, dissociative attachment, dissociative attachment with charge separation, single-electron transfer, dissociative single-electron transfer, and two-electron transfer. A qualitative description of the potential-energy profiles associated with these reaction channels is provided. The observed higher order chemistry of derivatized C_{60}^{n+} cations and of atomic exohedral adduct ions is also described. This chemistry includes cation-transfer reactions, surface derivatization, and "ball-and-chain" polymerization. Finally, results are presented that provide insight into the influence of surface strain on the reactivities of fullerene ions.

Key words: fullerenes, ions, electron transfer, charge separation, surface derivatization.

Résumé : On présente une revue des résultats de mesures récentes effectuées dans le « Ion Chemistry Laboratory at York University », utilisant la technique du tube à écoulement d'ions choisis (« SIFT »), pour des réactions des cations buckminsterfullerènes portant une, deux ou trois charges, C_{60}^{n+}, se produisant à la température ambiante, dans de l'hélium à 0,35 Torr agissant comme gaz tampon. Les coefficients de vitesse mesurés et les voies observées pour les produits de réactions avec une grande variété de molécules inorganiques et organiques dépendent fortement de la charge de l'ion qui réagit. Les coefficients de vitesse observés s'étalent sur quatre ordres de grandeur. Les principales voies observées pour les produits comprennent la fixation, la fixation dissociative, la fixation dissociative avec séparation de charge, le transfert d'un seul électron, le transfert dissociatif d'un seul électron et le transfert de deux électrons. On fournit une description qualitative des profils d'énergie potentielle reliées à ces voies réactionnelles. On décrit aussi la chimie d'ordre élevée observée pour les cations C_{60}^{n+} dérivatisés et pour les ions adduits exoédriques atomiques. Cette chimie inclut des réactions de transfert de cation, de dérivatisation en surface et de polymérisation en collier de perle avec bâtonnets. Enfin, on présente des résultats qui permettent de comprendre l'influence de la tension de surface sur les réactivités des ions fullerènes.

Mots clés : fullerènes, ions, transfert d'électron, séparation de charge, dérivatisation en surface.

[Traduit par la Rédaction]

1. Introduction

One of the many remarkable features of the isolated buckminsterfullerene molecule, C_{60}, is its stability as a multiply charged cation against Coulomb explosion. Tilmann Märk and his group at the University of Innsbruck have been able to produce and identify mass-spectrometrically C_{60} with up to 7 electrons removed from the ocean of 240 valence electrons that surround its hollow cage of 60 carbon atoms in this molecule (1). This has been achieved in a dedicated ion source that delivers high electron currents at high electron energies. In the Ion Chemistry Laboratory at York University we have found that it is straightforward to remove up to three electrons from C_{60} in the conventional electron-impact ion source that delivers ions into our selected-ion flow tube (SIFT) apparatus (2). The SIFT apparatus is a flow reactor designed to measure reaction-rate coefficients and product-ion distributions for reactions between gas-

Received March 26, 1999.

D.K. Böhme.[2] Department of Chemistry, York University, Toronto, ON M3J 1P3, Canada.

[1]This is an invited paper based on the 1998 J.C. Polanyi Award Lecture presented by Professor Böhme at the 81st Annual Conference of the Canadian Society for Chemistry in Whistler, British Columbia, June 1998.

[2]Telephone: (416) 736-2100, ext. 66188. Fax: (416) 736-5936. e-mail: dkbohme@yorku.ca

Fig. 1. Energy-level diagram for various charge states of C_{60}, a selection of singly charged atomic ions, and several rare-gas metastable atoms.

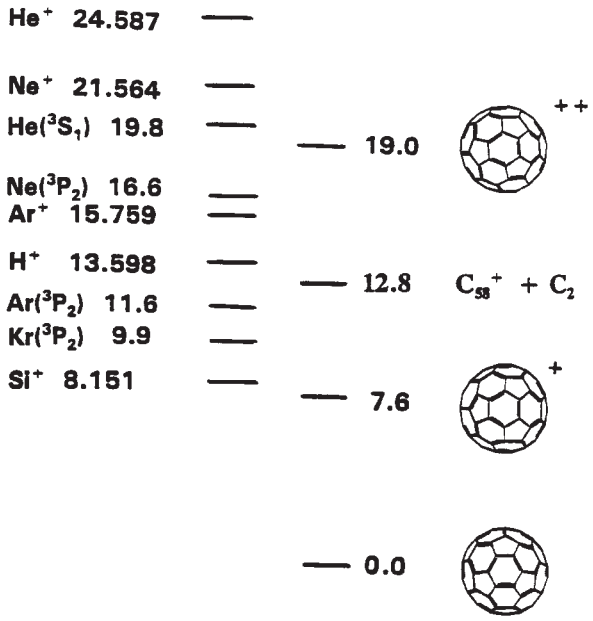

phase ions and neutral molecules. The ease of production of the first three ionized states of C_{60} has prompted us to explore systematically the uncharted chemistry of C_{60}^{n+} as a function of charge state from n = +1 to +3. Investigations of reactivity as a function of charge state are unprecedented in the greater world of gas-phase ion chemistry, in part because many molecular ions explode by intramolecular Coulombic repulsion already in the second charge state. We shall see in this overview that C_{60}^{n+} carbocations are extensively reactive in the gas phase at room temperature and more so as the charge state increases. New reaction pathways become accessible at higher degrees of ionization as, in a sense, physics increasingly preempts the occurrence of chemistry.

This overview is restricted to the research on the chemistry of fullerene ions performed in the author's own laboratory since 1991. No attempt has been made to review the larger body of gas-phase fullerene ion chemistry nor the gas-phase chemistry and physics of multiply charged ions generally that has been reported in the literature.

2. Electron transfer and chemi-ionization of C_{60}

Before embarking on measurements of the chemistry of C_{60}^{n+} ions, we first attempted the gas-phase ionization of C_{60} with methods other than electron-impact ionization. These early experiments showed that metastable atoms of He, Ne, Ar, and Kr induce the loss of electrons from C_{60} in the gas phase *at room temperature* in chemi-ionization (or Penning ionization) reactions of type [1] (3).

[1] $X^* + C_{60} \rightarrow C_{60}^+ + X + e$

Fig. 2. Schematic view of the Selected-Ion Flow Tube (SIFT) apparatus.

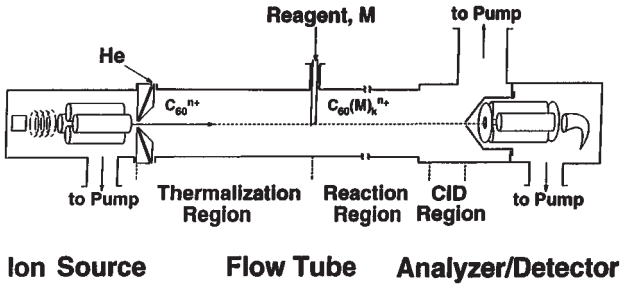

As shown in Fig. 1, these metastable atoms all have energies that lie above the first ionization energy of C_{60}, IE(C_{60}) = 7.61 ± 0.02 eV (4). The mechanism of reaction (1) can be understood in terms of the formation of an excited quasi-molecule $(XC_{60})^*$ that undergoes autoionization (3). We also found that C_{60} is readily ionized at room temperature in electron-transfer reactions of type [2] with ions that have a recombination energy (RE) larger than IE(C_{60}).

[2] $X^+ + C_{60} \rightarrow C_{60}^+ + X$

Such reactions have been observed in our laboratory with the atomic ions listed in Fig. 1 (5). While exothermic dissociative electron transfer leading to the rupture of C_{60}^+ through loss of C_2 was not observed to compete under our experimental operating conditions, we did see novel electron transfer/electron emission reactions of type [3] with X^+ = He^+ and Ne^+.

[3] $X^+ + C_{60} \rightarrow C_{60}^{2+} + X + e$

The mechanism of this novel reaction is not known. It has been suggested[3] that it proceeds by the initial transfer of a deeply embedded electron in C_{60} followed by an Auger emission of a second electron in a manner analogous to that which is known to occur when metals are exposed to slow beams of He^+ ions (6). The occurrence of reaction [3] may therefore be a manifestation of the metallic character of C_{60} due to the ocean of electrons that surround its hollow cage of 60 carbon nuclei.

3. The Selected-Ion Flow Tube (SIFT) apparatus

Our SIFT apparatus shown in Fig. 2 is essentially a tandem-quadrupole mass spectrometer in which the two quadrupoles are separated by a flow tube (2). Fullerene cations are generated in a conventional "open" electron-impact source at electron-impact energies from 60 to 100 eV, depending on the desired charge state: C_{60}^+ at ca. 50 eV, C_{60}^{2+} at ca. 80 eV, and C_{60}^{3+} at ca. 100 eV. The cations are selected upstream with the first quadrupole mass filter, injected through an aspirator-type inlet into He carrier gas at 0.35 Torr, allowed to thermalize to room temperature with ca. 10^5 collisions with He bath gas atoms, and then reacted with a desired reagent added into the flow tube. A large variety of stable gases and vapors of volatile liquids were added

[3] C.E. Klots. Private communication. 1993.

Fig. 3. Experimental data for the chemistry initiated by the reaction of $C_{60}^{\cdot 3+}$ with deuterated chloroform. $C_{60}^{\cdot 3+}$ was produced in a low-pressure ion source by electron impact at 100 eV with C_{60} vapour derived from a fullerene powder. The lines represent fits to the experimental data with solutions of the systems of differential equations appropriate for the observed reactions.

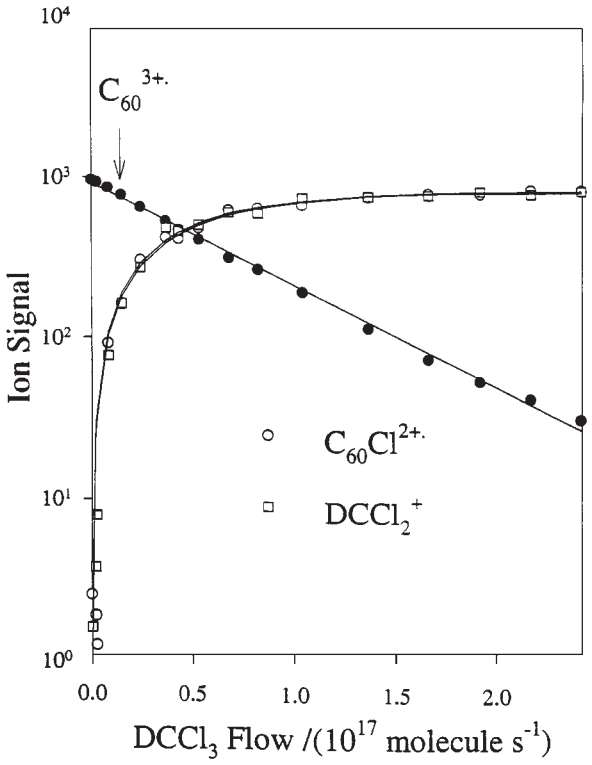

as reagents. Also, reagent hydrogen atoms were generated by the action of a microwave discharge upon a mixture of (5%) hydrogen and helium. The reacting mixture communicates with a second quadrupole mass spectrometer downstream and an electron multiplier, which monitor the reagent and product ions as a function of the flow of the neutral reagent. The reaction time is fixed at a few milliseconds by the buffer-gas flow velocity and the positions of the inlet and sampling ports.

Reaction profiles are obtained by monitoring reactant and product ions as a function of the flow of the neutral reagent. These profiles can be analyzed to provide rate coefficients for primary and secondary (or higher order) reactions as well as ion-product distributions. Representative reaction profiles for the chemistry initiated by C_{60}^{3+} in deuterated chloroform (7) are shown in Fig. 3. Bond connectivities in the product ions can be investigated in multicollision induced dissociation (CID) experiments by raising the sampling nose–cone voltage from 0 to –80 V while concomitantly varying the potentials of front and rear quadrupole focussing lenses so as not to introduce mass discrimination (8). The latter voltages are predetermined manually and then delivered with a programmable power supply.

Fig. 4. An overview of derivatization reactions of C_{60}^+ observed at a room temperature of 294 ± 2 K and a helium pressure of 0.35 ± 0.01 Torr. The assigned structures are speculative.

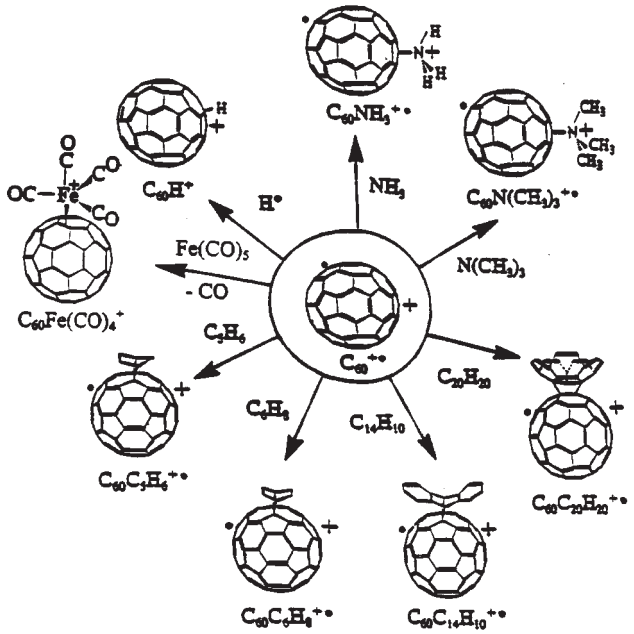

4. The chemistry of C_{60}^{n+} cations

A. Reactions of C_{60}^+

C_{60}^+ is generally quite nonreactive under SIFT conditions: we have found C_{60}^+ to be nonreactive towards more than 50 nonpolar, but also polar, inorganic and organic molecules. Electron transfer is rare because of the low electron-recombination energy of C_{60}^+ (7.6 eV (4)). The few chemical reactions of C_{60}^+ that we have observed so far under SIFT conditions are largely *termolecular* addition reactions that lead to chemical-bond formation with the carbonaceous surface of C_{60}^+. These are summarized in Fig. 4. We have found that C_{60}^+ can be derivatized with H atoms (9, 10), strong nucleophiles such as ammonia and aliphatic amines (11), and with molecules capable of Diels–Alder additions such as 1,3-cyclopentadiene, 1,3-cyclohexadiene, anthracene, and corannulene (12). A reaction of C_{60}^+ with iron pentacarbonyl produces $C_{60}Fe(CO)_4^+$ (13) and is the only example of a *bimolecular* derivatization reaction with C_{60}^+ that we have observed to date.

A remarkable trend is observed for the reactions of C_{60}^+ with amines: ammonia adds only slowly, but the rate of addition approaches the collision rate with increasing alkyl substitution. This behaviour is consistent with a trend in inductive electron donation (the Lewis basicity of the amine) and a trend in the number of degrees of freedom in the intermediate adduct ion effective in energy dispersal (11).

Here is how we envisage the progress of chemical reactions with singly charged C_{60}^+ (14). At long range the charge on the *isolated* cation, initially delocalized over the entire C_{60} surface, will become localized due to electrostatic interaction with the induced and (or) permanent dipole of the incoming molecule. Chemical attack at short separations should occur at the carbon site of a localized charge. For re-

Fig. 5. Schematic view of the increasing well depth of the potential-energy well leading to adduct formation, and of the barrier to covalent-bond formation in the double-well model, with increasing charge state.

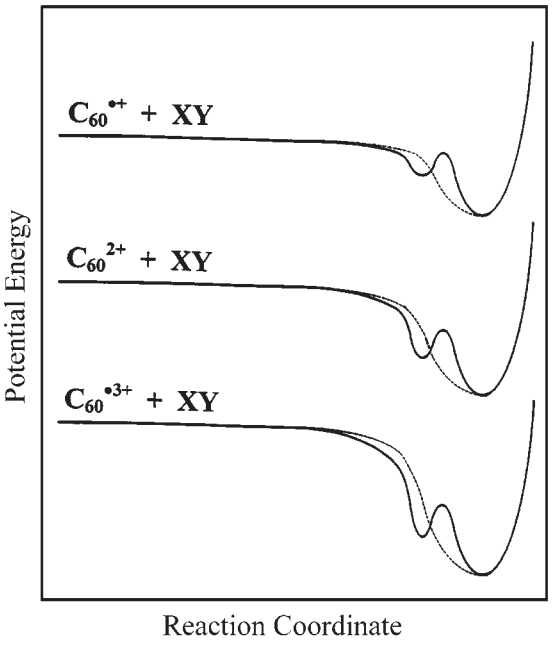

action to take place, a transition is required from largely sp^2 to largely sp^3 hybridization at the C-atom which becomes bonded. This requires surface deformation and so will involve an activation barrier that we estimate to be ca. 15 kcal mol^{-1}. Although this barrier can be overcome by electrostatic interaction with an incoming molecule, its presence can account for the relatively low reactivity of C_{60}^{+} at room temperature. The barrier is presumably located between the initial electrostatically bound complex and the ultimate chemically bound adduct, and should be easier to overcome if the electrostatic interaction is larger (see Fig. 5).

B. Reactions of C_{60}^{2+}

C_{60}^{2+} is much more reactive than C_{60}^{+} in both electron transfer and chemical bonding. We have attributed this enhanced reactivity to the higher recombination energy of C_{60}^{2+}, RE = 11.36 ± 0.05 eV (15), and to the stronger electrostatic interaction between molecules and C_{60}^{2+} that may serve to overcome the energy barrier associated with the change in hybridization required at the site of bonding (14), respectively. Figure 6 summarizes derivatization reactions observed with C_{60}^{2+}. The chemistry of C_{60}^{2+} has been explored with H atoms (9, 10), ammonia, and aliphatic amines (11), nitriles (16), water, alcohols, and ethers (17), aldehydes, ketones, carboxylic acids, and esters (18), cyclic aliphatic oxides (19), and unsaturated hydrocarbons (20–23). Electron transfer is an important competitive channel for

Fig. 6. An overview of derivatization reactions of C_{60}^{2+} observed at a room temperature of 294 ± 2 K and a helium pressure of 0.35 ± 0.01 Torr. The assigned structures are speculative.

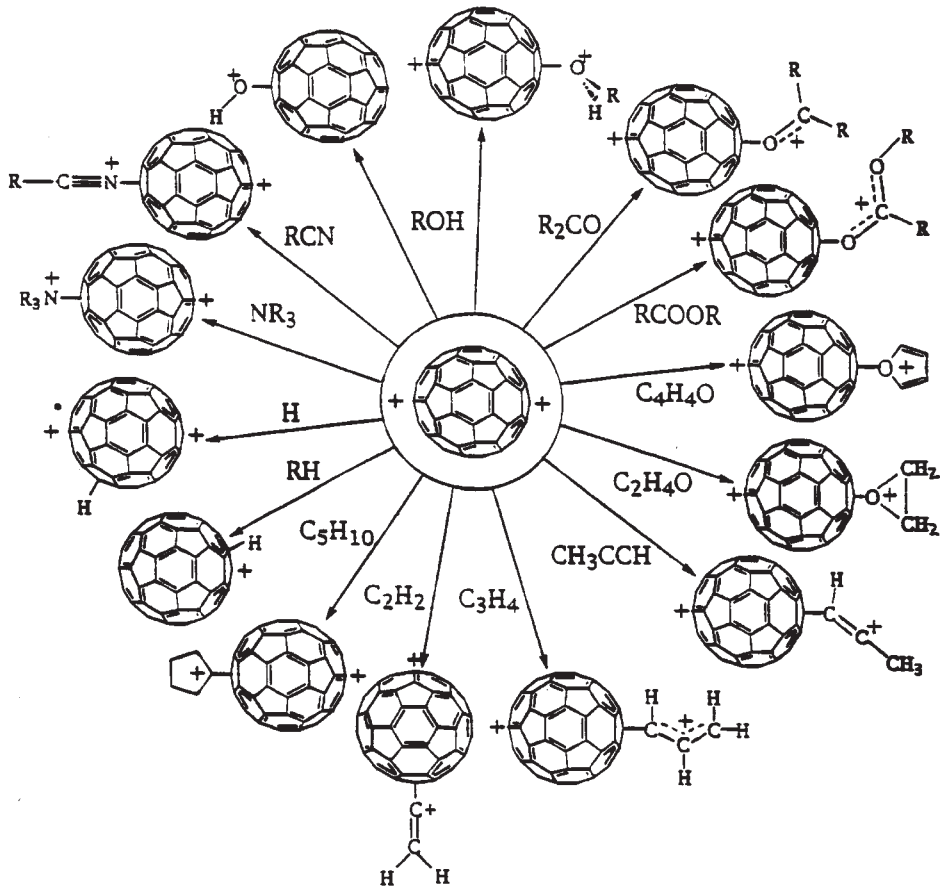

Fig. 7. Competition between electron transfer (broken line) and adduct formation (solid line) observed for reactions of C_{60}^{2+} with ammonia and amines at room temperature 294 ± 2 K and a helium pressure of 0.35 ± 0.01 Torr.

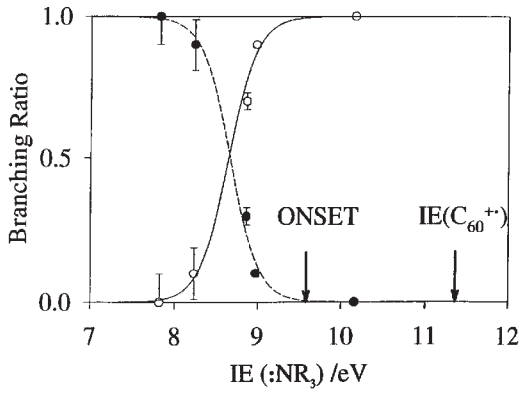

some of the observed derivatization reactions and, for molecules with sufficiently low ionization energies, becomes the only reaction channel. However, electron transfer with C_{60}^{2+} occurs in the presence of an activation barrier that arises from Coulomb repulsion between the charged product ions (24, 25). This is evident in Fig. 7 that shows a delayed onset for competing electron transfer at about 9.6 eV, which is well below the recombination energy of C_{60}^{2+} (11.36 ± 0.05 eV). Electron transfer must be exothermic by at least 1.8 eV in order to compete effectively.

C. Reactions of C_{60}^{3+}

Derivatization reactions also have been observed with C_{60}^{3+}, but electron transfer is even more competitive than with C_{60}^{2+}. For example, although we have observed ammonia to add to C_{60}^{3+}, only electron transfer has been seen with amines (11). The ionization-energy threshold for electron transfer to C_{60}^{3+} lies 4.4 eV below the thermodynamic threshold of RE (C_{60}^{3+}) = 15.6 eV (15). This threshold is higher in energy than observed for electron transfer to C_{60}^{2+} and again can be rationalized in terms of an energy barrier arising from Coulombic repulsion between the product ions (24, 25). We have also observed C_{60}^{3+} cations to abstract *two* electrons from corannulene and the PAH molecules anthracene, pyrene, and benzo[*rst*]pentaphene in reactions of type [4] (26).

$$[4] \qquad C_{60}^{3+} + M \rightarrow M^{2+} + C_{60}^{+}$$

All of these PAH molecules have sufficiently low first and second ionization energies to make double-electron transfer thermodynamically and kinetically favourable. The mechanism of the two-electron transfer reaction [4], whether electron transfer is concomitant or sequential, is not known. Reaction [4] occurs in competition with single-electron transfer. It was observed as a minor channel (<5%) with anthracene, corannulene, and pyrene and occurs in almost equal amounts with benzo[*rst*]pentaphene, which requires the lowest energy for double ionization of these four PAH molecules. The single and two-electron transfer observed with corannulene is illustrated in eq. [5]. (The structure of corannulene is assumed not to change upon ionization.)

[5]

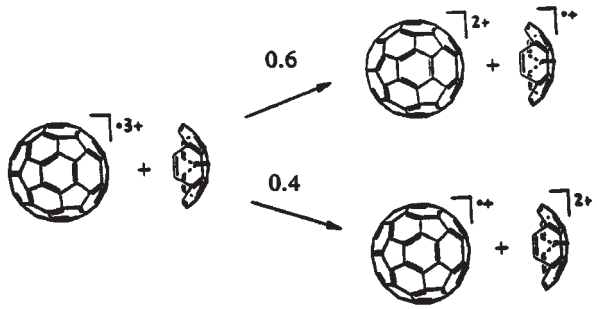

Reactions of C_{60}^{3+} have been investigated with H atoms (9, 10), nitriles (16), water, alcohols, and ethers (17), aldehydes, ketones, carboxylic acids, and esters (18), cyclic aliphatic oxides (19), and unsaturated hydrocarbons (20–23). Figure 8 provides a summary of addition reactions observed. New, charge separation, channels appear for some of the reactions with C_{60}^{3+}. For example, dissociative electron transfer to produce $C_{60}^{2+}/CH_2NH_2^+$ and C_{60}^{2+}/CH_3^+ is the dominant reaction channel with ethylamine [12]. Also, dissociative addition reactions such as hydride and hydroxide transfer, become more effective. This is the case with water, some alcohols, and some alkanes. Halide transfer from HCl and HBr also has been observed. HCl reacts both by Cl^- transfer to produce, remarkably, a free proton as the second ion product (88%) and by hydride transfer (12%) according to reaction [6]. HBr also reacts by halide transfer, but the competing channel in this case is dissociative electron transfer (27).

$$[6a] \qquad C_{60}^{3+} + HCl \rightarrow C_{60}Cl^{2+} + H^+$$

$$[6b] \qquad \rightarrow C_{60}H^{2+} + Cl^+$$

5. Trends with charge state

Reactions [7*a*]–[7*f*] summarize the various types of reactive encounters we have observed between the first three charge states of C_{60}^{n+} and some 30 different reactive molecules that we have surveyed. These include addition [7*a*], dissociative addition [7*b*], dissociative addition with charge separation [7*c*], single-electron transfer [7*d*], dissociative single-electron transfer [7*e*], and two-electron transfer [7*f*].

$$[7a] \qquad C_{60}^{n+} + XY \rightarrow C_{60}XY^{n+}$$

$$[7b] \qquad \rightarrow C_{60}X^{n+} + Y$$

$$[7c] \qquad \rightarrow C_{60}X^{(n-1)+} + Y^+$$

$$[7d] \qquad \rightarrow C_{60}^{(n-1)+} + XY^+$$

$$[7e] \qquad \rightarrow C_{60}^{(n-1)+} + X^+ + Y$$

$$[7f] \qquad \rightarrow C_{60}^{(n-2)+} + XY^{2+}$$

Both the nature of the product channel and the rate of reaction were observed to be a function of the charge state of C_{60}^{n+}. This is indicated qualitatively in Fig. 9. A unified model for these reactive encounters in terms of schematic potential-energy profiles is given in Fig. 10 (28). An analogous model was originally introduced by Herman (29) to account for the observed reactivities of other, smaller doubly

Fig. 8. An overview of derivatization reactions of C_{60}^{3+} observed at a room temperature of 294 ± 2 K and a helium pressure of 0.35 ± 0.01 Torr. The assigned structures are speculative.

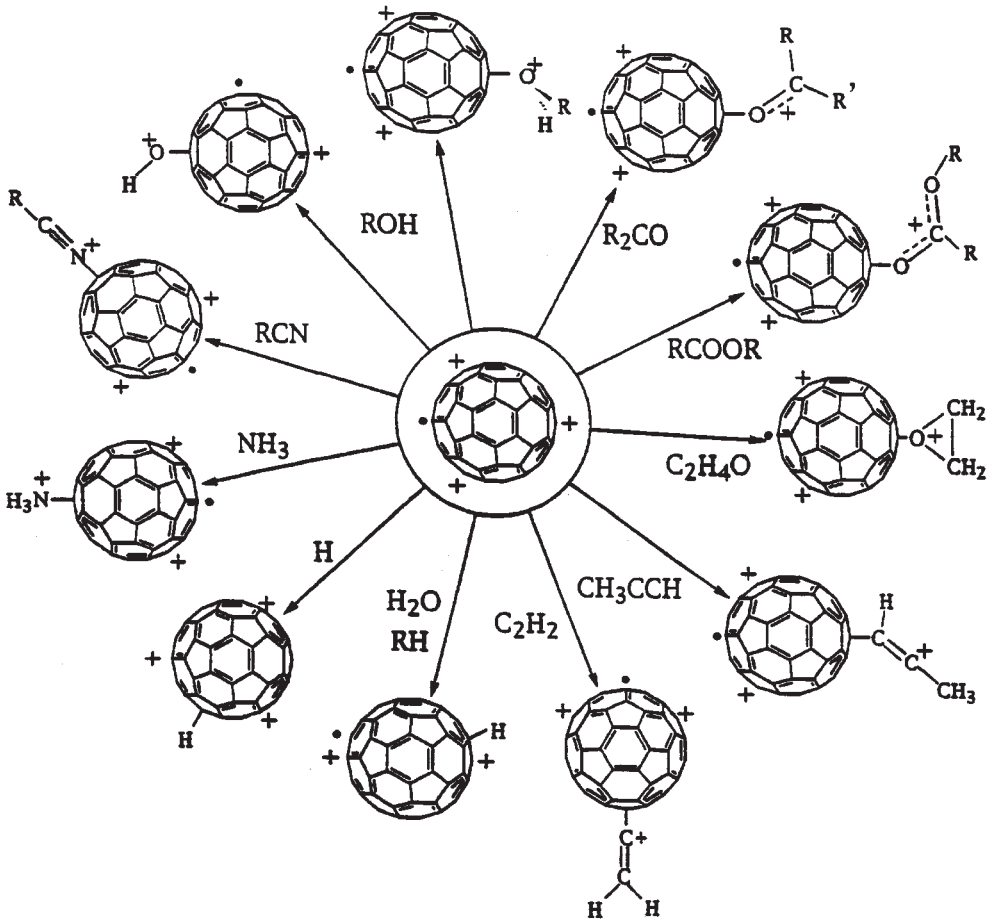

Fig. 9. Qualitative overview of the trend in the reactivity of C_{60}^{n+} cations with charge state. The predominant reaction channels that were observed are indicated in the order of general importance. RE is the recombination energy.

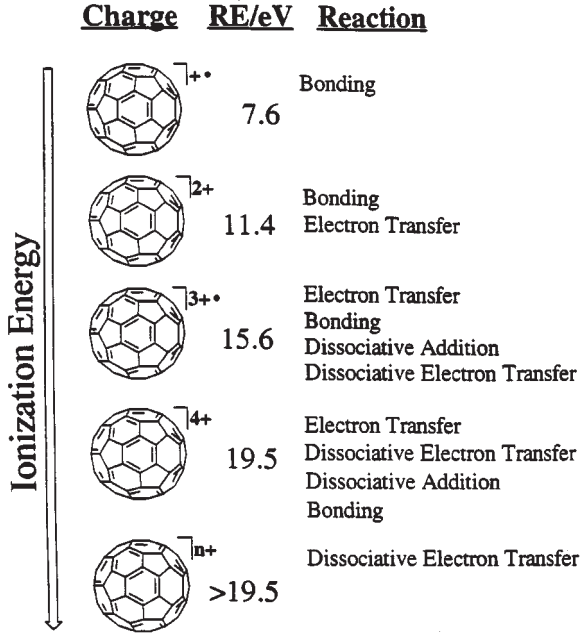

charged ions. As reactants approach each other within this model, a multiply charged fullerene cation encounters single, double, and dissociative electron-transfer potential-energy curve crossings first whereupon a nonadiabatic transition may occur leading to the transfer of an electron. Those C_{60}^{n+}-M pairs that survive the electron-transfer crossings may undergo inelastic collisions with He buffer-gas atoms to produce stable adduct ions $C_{60}M^{n+}$. Failing that, bond redisposition may occur by dissociative addition with or without charge separation. The opportunity for electron transfer increases with increasing charge state. In a sense, chemistry is increasingly preempted by physics with increasing charge state.

6. Higher order chemistry

We have shown that C_{60}^{n+} cations may be derivatized in primary addition or dissociative addition reactions of types [7*a*], [7*b*], and [7*c*]. Now we explore the higher order chemistry of these derivatized ions. Figure 11 provides an overview of this chemistry.

A. Cation-transfer reactions

A number of secondary reactions have been observed with derivatized fullerene cations that involve the transfer of a

Fig. 10. Summary of plausible potential-energy profiles for reactions [6*a*]–[6*f*] as a function of charge state. The minima in these profiles represent bound adducts $C_{60}M^{n+}$. The repulsive curves on the left represent charge separation channels corresponding to single, double, and dissociative electron transfer. Those on the right represent bond formation by dissociative addition with or without charge separation.

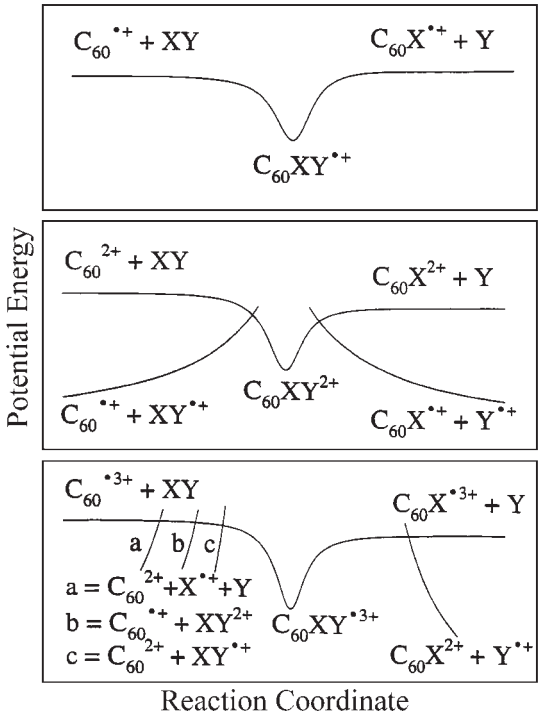

proton, a methyl cation, or the entire ionized substituent. When the substituent contains a hydrogen atom, $C_{60}XH^{n+}$ may undergo partial or complete proton transfer with a suitable proton acceptor. Thus, secondary reactions of singly charged $C_{60}XH^{+}$ ions produce proton-bound adducts of the type $C_{60}X\cdots H^{+}\cdots XH$ with XH = NH_3, CH_3NH_2, $C_2H_5NH_2$, and $(CH_3)_2NH$ (13). Doubly charged derivatized $C_{60}(XH)_m^{2+}$ (m = 1, 2) cations have been observed to undergo rapid proton-transfer reactions of type [8] with XH = ammonia, amines, alcohols, carboxylic acids, ketones, and cyanides (30).

[8] $C_{60}(XH)_m^{2+} + XH \rightarrow C_{60}(XH)_{m-1}X^{+} + XH_2^{+}$

Reaction [9] provides one example of such a proton transfer for XH = NH_3 and m = 1.

[9]

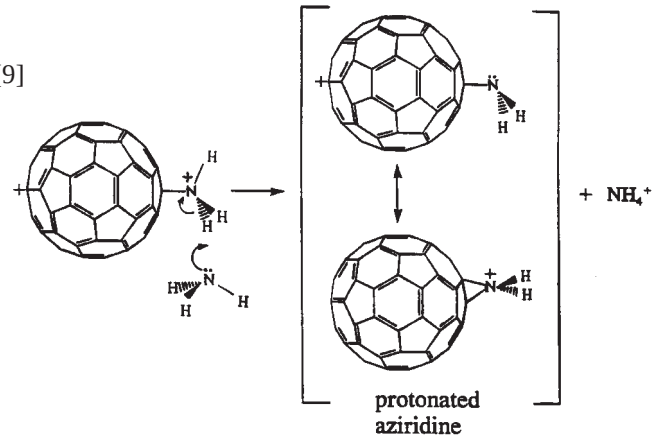

We have assessed this proton-transfer reactivity in terms of an apparent gas-phase acidity of the dicationic species $C_{60}(XH)_m^{2+}$ and have taken the first steps towards establishing a gas-phase acidity ladder for derivatized fullerene cations (30). Also, we have established the gas-phase acidity of $C_{60}H^{2+}$ from the occurrence and nonoccurrence of proton-transfer reactions with this cation (31).

Reactions with methyl formate and methyl acetate involve the transfer of a methyl cation according to eq. [10] proceeding in competition with adduct formation and proton transfer (18).

[10] $C_{60}(XCH_3)^{3+} + XCH_3 \rightarrow C_{60}(X)^{2+} + X(CH_3)_2^{+}$

Fig. 11. Overview of the higher order chemistry of C_{60} adduct ions, designated as $C_{60}AB^{n+}$, with molecules M.

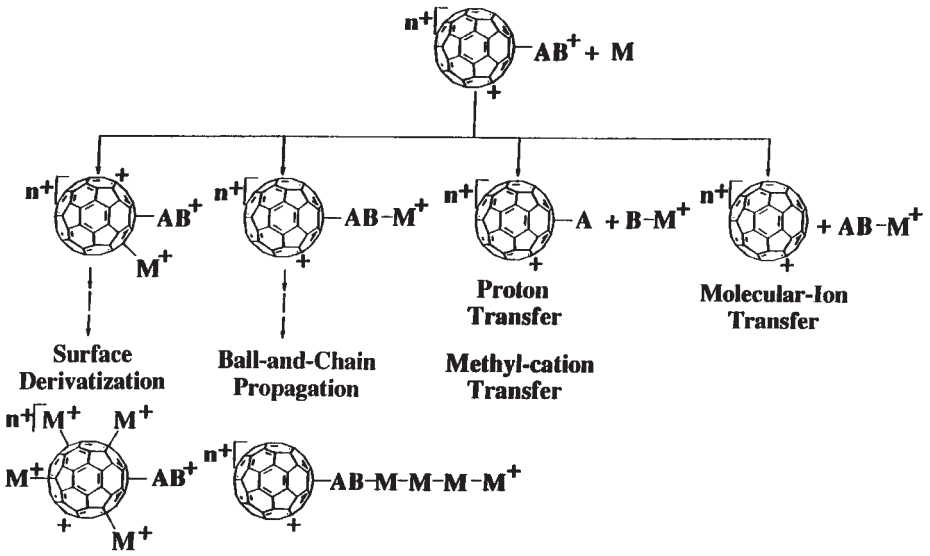

Fig. 12. Variation in the rate coefficient measured for the sequential methoxylation reaction of C_{60}^{2+} with methyl nitrite at room temperature in helium buffer gas at 0.35 Torr.

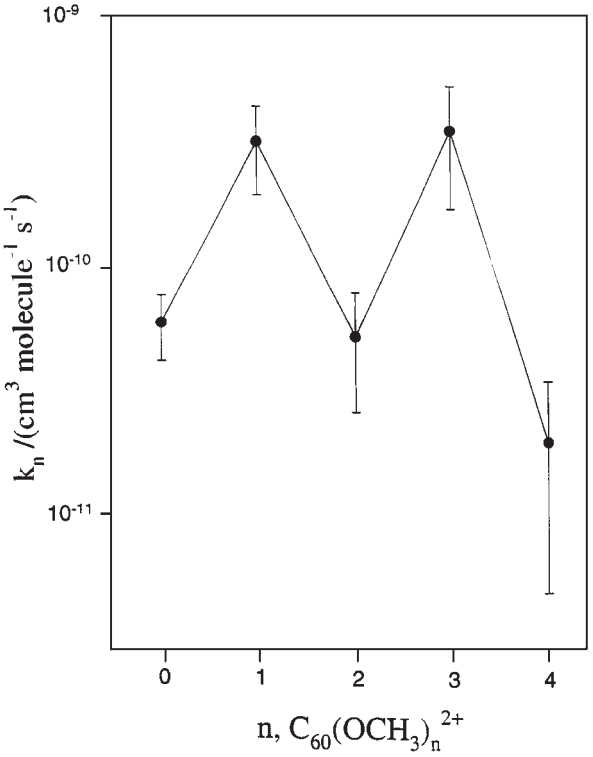

Also, we have observed several reactions of derivatized fullerene cations that involve the complete transfer of the ionized substituent according to eq. [11] with R = CN, C_2H_3, C_3H_3, and CH_2CN (16).

[11] $C_{60}(NCR)^{3+} + RCN \rightarrow C_{60}^{2+} + (RCN)_2^+$

Presumably such reactions are driven by the stability of the product dimer cation.

B. Surface derivatization

A number of higher order reactions have been observed in our laboratory that result in the sequential derivatization of the *surface* of the fullerene cation to produce what have been called "fuzzy ball" structures. H atoms were seen to add sequentially to the first three charge states of C_{60}^{n+} to produce $C_{60}H_m^{n+}$ according to reaction [12], with *m* up to 9 and constrained only by the number density of H atoms that we were able to generate in the flow tube experimentally (8, 9).

[12] $C_{60}H_m^{n+} + H \rightarrow C_{60}H_{m+1}^{n+}$

Several aliphatic nitriles have been observed to add rapidly to C_{60}^{n+} in numbers equal to the number of charges on C_{60}^{n+} to produce adducts according to reaction [13], with *n* up to 4 (16).

[13] $C_{60}(NCR)_m^{n+} + RCN \rightarrow C_{60}(NCR)_{m+1}^{n+}$

These adducts have the following plausible structures (16).

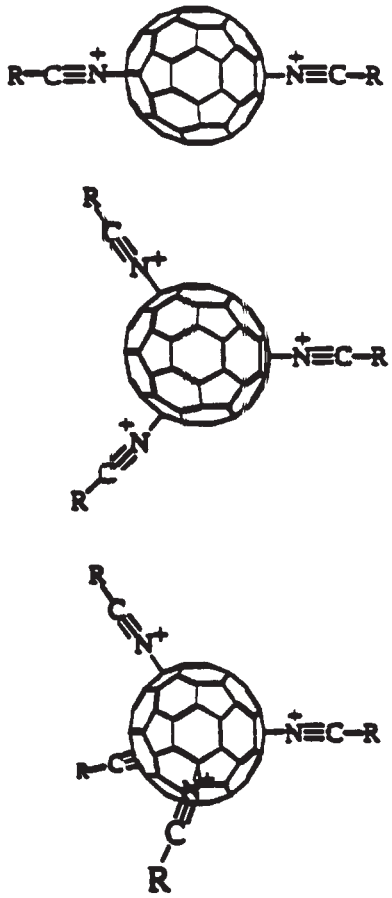

Also, C_{60}^{2+} has been observed to react with methyl nitrite in sequential bimolecular reactions leading to the sequential transfer of at least 15 methoxy groups according to reaction [14] (31).

[14] $C_{60}(CH_3O)_m^{2+} + CH_3ONO \rightarrow C_{60}(CH_3O)_{m+1}^{2+} + NO$

The addition kinetics exhibits periodicities of 2 and 4 that have been attributed to periodicities in the stabilities of the resulting surface-derivatized cations of which the following structure is representative.

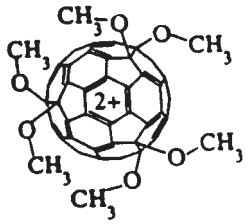

The occurrence of surface derivatization was deduced from observations of the collision-induced dissociation of the $C_{60}(CH_3O)_{m+1}^{2+}$ product ions that indicated loss of a single CH_3O group for all values of *m*. The periodicity in reaction rate is shown in Fig. 12. The higher reactivities of the odd-numbered $C_{60}(CH_3O)_m^{2+}$ adduct ions have been attributed to their radical nature. The lower reactivities of the 4th and 8th adducts have been ascribed to an aromatic character for these cations as they contain $(4n + 2)$ π electrons (32).

Fig. 13. Data for the sequential addition of allene to C_{60}^{2+} observed at a room temperature of 294 ± 2 K and a helium pressure of 0.35 ± 0.01 Torr.

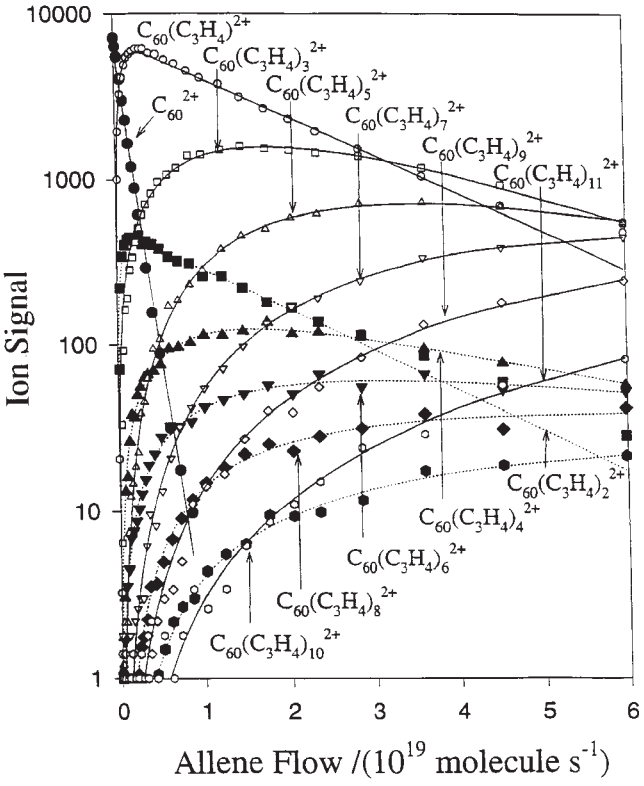

Fig. 14. Measured profiles for the multicollision-induced dissociation of $C_{60}(allene)^{2+}$ at an allene flow of 4.5×10^{19} molecules s^{-1} in 10% argon–helium at a total pressure of 0.30 ± 0.01 Torr and 294 ± 2 K.

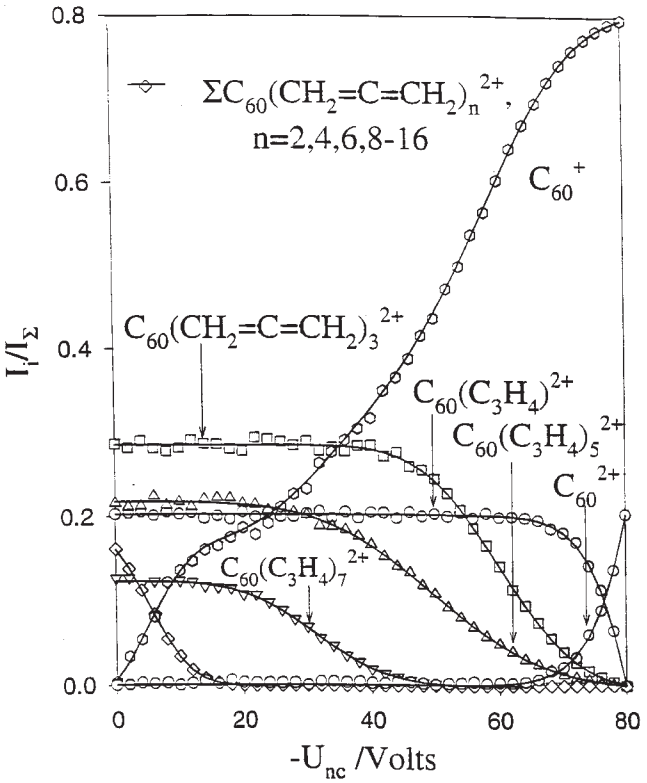

C. Ball-and-chain propagation

With some molecules we have observed multiple derivatization that we suggest leads to chain propagation or ball-and-chain formation in the manner indicated by reaction [15].

[15] 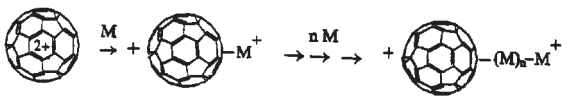

We have proposed such reactions for C_{60}^{2+} reacting sequentially with ethylene (33), propene, allene (33), 1,3-butadiene (21), *cis*, and *trans*–1,3-pentadiene, acetylene (33), methyl acetylene (34), diacetylene, cyanoacetylene, ethylene oxide (19), and propylene oxide. Many of these molecules are well known as monomers in traditional polymer chemistry. Indeed, reaction [15] may be regarded as an ion-induced polymerization reaction. A noteworthy feature of reaction [15] is the concomitant intramolecular charge separation. We have postulated that one of the charges is propagated along the substituent driven by Coulombic repulsion, which directs chain growth away from the C_{60} surface (21).

The chemistry of C_{60}^{2+} and allene is of particularly interest, since the sequential addition exhibits a striking periodicity in reactivity, with the *even*-numbered adducts reacting about 10 times faster than the *odd*-numbered adducts (see Fig. 13). We have managed to probe the bond connectivity in these adducts using multicollision induced dissociation. Figure 14 shows that the first allene molecule comes off intact by *heterolytic* dissociation to regenerate the C_{60}^{2+} dication. Higher adducts appear to completely eliminate polymers of allene in one step by *homolytic* dissociation, leading to charge separation and formation of singly charged C_{60}^{+}. Also, Fig. 14 shows that the odd adducts have a higher stability than the even adducts, which exhibit a much lower threshold for dissociation. Taken together, the kinetic and collision-induced dissociation results have led us to propose a mechanism involving the alternating formation of *charge-localized even-numbered acyclic allyl cations*,which can be expected to be more reactive, and the formation of *charge-delocalized cyclic odd-numbered allyl cations*, which would be less reactive. The following semi-empirical MP3 structure calculated for $C_{60}(allene)_7^{2+}$ is representative of an odd-numbered allyl cation.

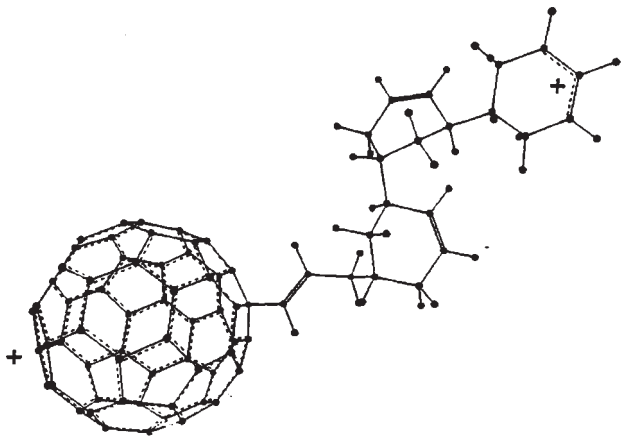

Fig. 15. Experimental data for the reaction of $C_{60}Fe^+$ with CO in helium buffer gas at a total pressure of 0.30 ± 0.01 Torr and 294 ± 2 K. The fifth adduct, $C_{60}Fe(CO)_5^+$ could not be detected.

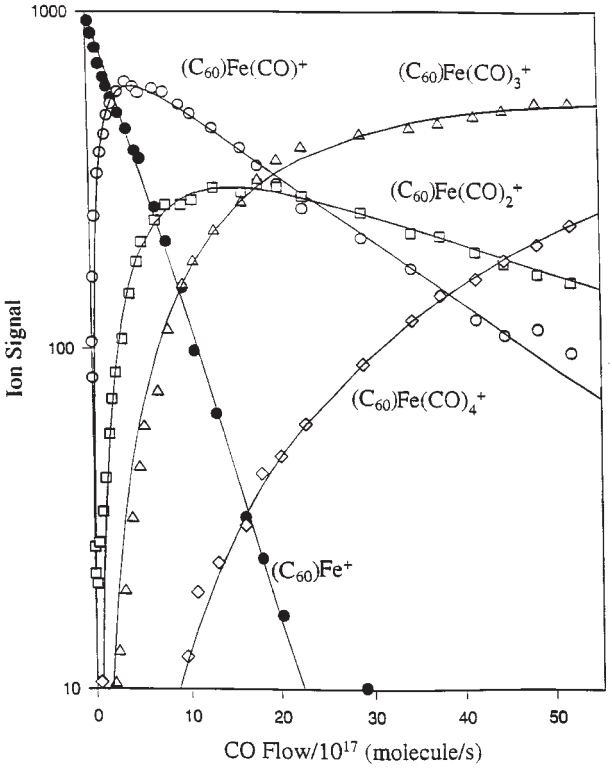

7. Reactions of atomic exohedral adduct ions

Recently we have become interested in elucidating the influence of C_{60} as a ligand on the reactivity of metal ions. Atomic ions readily can be attached to C_{60} upstream in the flow tube of our SIFT apparatus by attachment reactions of type [16], and the chemistry of the adduct ion then can be followed downstream.

[16] $A^+ + C_{60} + He \rightarrow C_{60}A^+ + He$

For example, we have already observed the attachment of Si^+, Fe^+, and Mg^+ to C_{60} under SIFT conditions. Questions arise regarding the nature of the bonding in $C_{60}A^+$ and the location of A^+ on the C_{60} surface. Possible sites for the location of Fe^+ on the C_{60} surface are illustrated below.

We hypothesized that a comparative study of the chemical reactivity of Fe^+ ligated to C_2H_4, *c*-C_5H_5, C_6H_6, and C_{60} would provide insight into the mode of bonding in $C_{60}Fe^+$. Indeed, reactivity measurements with CO and N_2O indicated a match between $(C_2H_4)Fe^+$ and $C_{60}Fe^+$ that suggests that the $(\eta^2\text{-}C_{60})Fe^+$ structures are preferred for $C_{60}Fe^+$ generated under SIFT conditions (35).

A comparison of the reactivities of $C_{60}Fe^+$ and the unligated Fe^+ ion provides a measure of the influence of the C_{60} ligand on chemical reactivity. Thus the addition reaction of CO with Fe^+, which does not occur measurably for the isolated cation ($k < 10^{-14}$ cm^3 molecule^{-1} s^{-1}), proceeds rapidly in the presence of C_{60} ($k = 1.3 \times 10^{-10}$ cm^3 molecule^{-1} s^{-1}). Three more molecules add sequentially (see Fig. 15), presumably to the Fe center according to reaction [17].

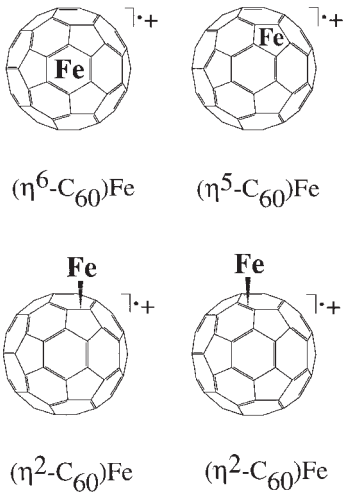

[17]

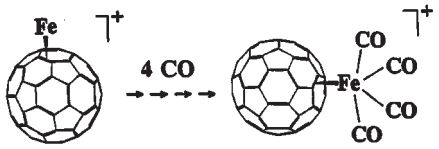

Also, the rate of the bimolecular O-atom transfer reaction of nitrous oxide with Fe^+ ($k = 3.1 \times 10^{-11}$ cm^3 molecule^{-1} s^{-1}) is enhanced by a factor of more than three in the presence of C_{60} ($k = 1.0 \times 10^{-10}$ cm^3 molecule^{-1} s^{-1}). Again, the O-atom transfer presumably occurs at the Fe site as shown in reaction [18].

[18]

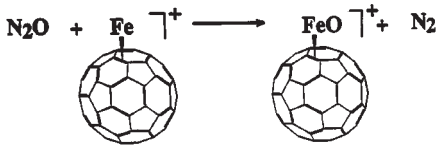

8. On the influence of surface strain on the reactivities of fullerene ions

Fullerene molecules, and presumably also their ions, provide a range of reactive C sites with different degrees of hybridization and strain (36). We have made some progress in investigating the influence of such surface features on the chemical reactivity of fullerene cations. Our early investigations of addition reactions of fullerene cations C_{56}^+, C_{58}^+, and C_{60}^+ with NH_3, of addition reactions of C_{56}^{2+}, C_{58}^{2+}, and C_{60}^{2+} with C_2H_4 and CH_3CN, and of hydride-transfer reactions of C_{56}^{2+}, C_{58}^{2+}, and C_{60}^{2+} with *n*-C_4H_{10}, revealed an enhanced reactivity for the adjacent-pentagon fullerene ions of C_{56} and C_{58} relative to those of C_{60} (37). Adjacent pentagons enhance the curvature of the carbon surface and the sp^3 character of selected C sites (37). More recent systematic studies of addition reactions of C_{56}^+, C_{58}^+, C_{60}^+, C_{70}^+, corannulene$^+$, and coronene$^+$ with cyclopentadiene and 1,3-cyclohexadiene indicated that the efficiency of bond forma-

Fig. 16. Semi-logarithmic plot for the dependence of reaction efficiency on the square of the POAV angle and the strain energy for reactions with cyclopentadiene in helium buffer gas at 0.35 Torr and 294 ± 2 K. k_{obs} is the measured rate coefficient and k_c is the collision rate coefficient, which is estimated to be 10^{-9} cm^3 molecule^{-1} s^{-1}. The horizontal bars represent the range in strain energy presented by the various cations, which could not be resolved, since the exact C site(s) being bonded could not be determined.

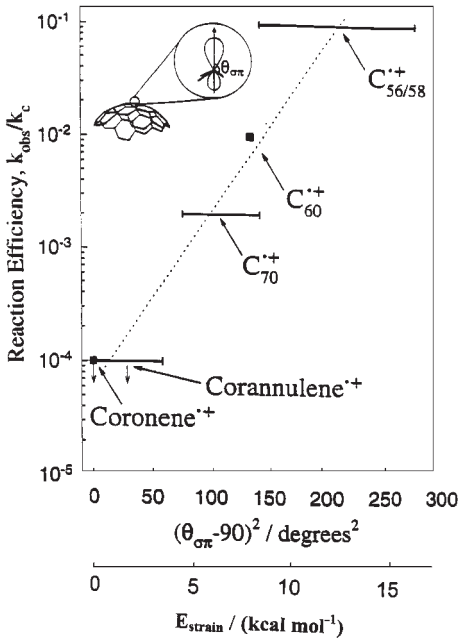

Table 1. POAV angles for various sites on selected carbonaceous molecules.

POAV angle, θ_x (deg)	C_{60}	C_{70}	Corannulene	Coronene
θ_1	11.6[a]	12.0[a]	7.7[b] (8.2)[c]	0
θ_2	—	11.9[a]	3.0[b] (3.8)[c]	0
θ_3	—	11.5[a]	0	0
θ_4	—	10.0[a]	—	—
θ_5	—	8.9[a]	—	—

[a]Reference 39.
[b]Reference 40.
[c]Reference 41.

tion with these two molecules also depends strongly on the curvature of the carbonaceous surface of the reacting cation (38).

On a carbonaceous surface the strain energy will depend upon the π orbital axis vector (POAV) angle, θ (36): the angle between the π-orbital at the bonding C site and one of the σ bonds on the adjacent carbonaceous surface minus 90° (see Fig. 16). For a planar sp^2 carbon atom this angle is 0°, and for a tetrahedral sp^3 carbon atom it is 19.47°. The POAV angles for the different sites in C_{60} and C_{70} and the related corannulene and coronene molecules shown below are given in Table 1. C_{70} has five different types of C sites with different surface strain, while C_{60} has only one such site. There is no strain in the flat PAH coronene whereas the bowl-shaped corannulene molecule has three types of C sites including one without strain.

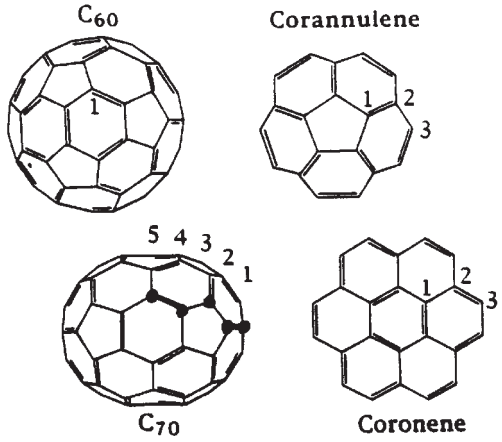

Figure 16 shows that the Diels–Alder addition with cyclopentadiene is faster with the smaller, more strained fullerenes and that the efficiencies of addition to the less-strained corannulene cation and the flat coronene cation are immeasurably small. Apparently the addition is driven by the relief of strain energy. The correlation presented in Fig. 16 leads to the following approximate dependence of the rate coefficient for addition on strain energy *E*, in kcal mol^{-1}, over the range in POAV angle explored.

[19] $k = 6.0 \times 10^{-14}\ e^{0.595E}$

These results also suggest a preference in reactivity for C sites with the highest strain energy (or the site with the highest local curvature) in those cations with more than one site of different strain as is the case, for example, with C_{70}^+ and corannulene$^+$. Such regioselectivity has been identified in earlier solution studies of the osmylation of C_{70} (42).

Conclusions

I have surveyed here much of the remarkable chemistry of buckminsterfullerene cations that has been revealed by our laboratory measurements using the SIFT technique since we began our studies in 1991. The charge state of C_{60}^{n+} has been shown to be decisive in determining the nature of this chemistry. Multiple derivatization, both of the C_{60} surface and in a ball-and-chain fashion, is an important feature of the higher order chemistry, particularly in the chemistry initiated by C_{60}^{2+} and C_{60}^{3+}. But, as the electron recombination energy of C_{60}^{n+} increases with increasing ionization, the transfer of one or more electrons from a reacting molecule eventually dominates.

Singly charged fullerene ions are known to be produced naturally in certain hydrocarbon flames where they have been shown to add hydrogen atoms (43). We have proposed elsewhere that mechanisms exist for the production of singly and doubly charged fullerenes from neutral fullerenes thought to be present in interstellar clouds and circumstellar atmospheres (44). The chemistry of these fullerene ions may have important consequences in these environments. For example, additions of hydrogen atoms to ionized fullerenes

that we have observed under SIFT conditions are expected to be efficient and may lead to the production of *fulleranes* (hydrogenated fullerenes) upon neutralization or even to the formation of molecular hydrogen by hydrogen-atom recombination on the fullerene-ion surface. Furthermore, additions of a variety of other known interstellar and circumstellar atoms and molecules to ionized fullerenes, particularly to doubly charged fullerenes, as well as additions of ions to neutral fullerenes are also likely. Finally, our results in the gas phase for the chemistry of C_{60}^{n+} should serve as a useful benchmark for the chemistries of fullerene cations in solution. These chemistries have not yet been elucidated, although persistent singly and multiply charged cations of C_{60} and other fullerenes have been observed in solution (45–47).

Acknowledgements

A number of graduate students and postdoctoral fellows have participated in the fullerene-ion research over the years, and I am grateful for their contributions. Special thanks go to Dr. Simon Petrie, Dr. Reza Javahery, and Dr. Vladimir Baranov for their inspiring collaboration. Also, I wish to thank the Natural Sciences and Engineering Research Council of Canada for ongoing financial support and the Canada Council for a Killam Research Fellowship during the formative part of this research.

References

1. P. Scheier, B. Dünser, R. Wörgötter, S. Matt, D. Muigg, G. Senn, and T.D. Märk. Int. Rev. Phys. Chem. **15**, 93 (1996).
2. G.I. Mackay, G.D. Vlachos, D.K. Böhme, and H.I. Schiff. Int. J. Mass Spectrom. Ion Phys. **36**, 259 (1980).
3. G. Javahery, S. Petrie, J. Wang, X. Wang, and D.K. Böhme. Int. J. Mass Spectrom. Ion Processes **125**, R13 (1992).
4. D.L. Lichtenburger, M.E. Rempe, and S.B. Gogosha. Chem. Phys. Lett. **198**, 454 (1992).
5. G. Javahery, S. Petrie, J. Wang, and D.K. Böhme. Chem. Phys. Lett. **195**, 76 (1992).
6. H.D. Hagstrum. Phys. Rev. **96**, 336 (1954).
7. Y. Ling, G.K. Koyanagi, D. Caraiman, V. Baranov, and D.K. Böhme. Int. J. Mass Spectrom. **192**, 215 (1999).
8. V. Baranov and D.K. Böhme. Int. J. Mass Spectrom. Ion Processes, **154**, 71 (1996).
9. S. Petrie, G. Javahery, J. Wang, and D.K. Böhme. J. Am. Chem. Soc. **114**, 6268 (1992).
10. S. Petrie, H. Becker, V.I. Baranov, and D.K. Böhme. Int. J. Mass Spectrom. Ion Processes, **145**, 79 (1995).
11. G. Javahery, S. Petrie, H. Wincel, J. Wang, and D.K. Böhme. J. Am. Chem. Soc. **115**, 5716 (1993).
12. H. Becker, G. Javahery, S. Petrie, and D.K. Böhme. J. Phys. Chem. **98**, 5591 (1994).
13. V. Baranov and D.K. Böhme. Int. J. Mass Spectrom. Ion Processes, **165**/**166**, 249 (1997).
14. S. Petrie and D.K. Böhme. Can. J. Chem. **72**, 577 (1994).
15. D.K. Böhme. Int. Rev. Phys. Chem. **13**, 163 (1994).
16. G. Javahery, S. Petrie, J. Wang, H. Wincel, and D.K. Böhme. J. Am. Chem. Soc. **115**, 9701 (1993).
17. G. Javahery, S. Petrie, H. Wincel, J. Wang, and D.K. Böhme. J. Am. Chem. Soc. **115**, 6295 (1993).
18. S. Petrie, G. Javahery, H. Wincel, J. Wang, and D.K. Böhme, Int. J. Mass Spectrom. Ion Processes, **138**, 187 (1994).
19. J. Wang, G. Javahery, S. Petrie, A.C. Hopkinson, and D.K. Böhme. Angew. Chem. Int. Ed. Engl. **33**, 206 (1994).
20. J. Wang, G. Javahery, S. Petrie, and D.K. Böhme. J. Am. Chem. Soc. **114**, 9665 (1992).
21. J. Wang, V. Baranov, and D.K. Böhme. J. Am. Soc. Mass Spectrom. **7**, 261 (1996).
22. J. Wang, G. Javahery, V. Baranov, and D.K. Böhme. Tetrahedron, **52**, 5191 (1996).
23. V. Baranov, J.Wang, A.C. Hopkinson, and D.K. Böhme. J. Am. Chem. Soc. **119**, 2040 (1997).
24. S. Petrie, J. Javahery, J. Wang, and D.K. Böhme. J. Phys. Chem. **96**, 6121 (1992).
25. S. Petrie, G. Javahery, J. Wang, and D.K. Böhme. J. Am. Chem. Soc. **114**, 6268 (1992).
26. G. Javahery, H. Becker, S. Petrie, P.C. Cheng, H. Schwarz, L.T. Scott, and D.K. Böhme. Org. Mass Spectrom. **20**, 1005 (1993).
27. V. Baranov and D.K. Böhme. Chem. Phys. Lett. **258**, 203 (1996).
28. D.K. Böhme. *In* Recent advances in the chemistry and physics of fullerenes and related materials.. Electrochem. Soc. Proc. Vol. 97-14. *Edited by* R.S. Ruoff and K.M. Kadish. Electrochemical Society, Inc., Pennington, N.J. 1997. p. 763.
29. Z. Herman. Int. Rev. Phys. Chem. **15**, 299 (1996).
30. S. Petrie, G. Javahery, and D.K. Böhme. Int. J. Mass Spectrom. Ion Processes, **124**, 145 (1993).
31. S. Petrie, G. Javahery, H. Wincel, and D.K. Böhme. J. Am. Chem. Soc. **113**, 6290 (1993).
32. V. Baranov, A.C. Hopkinson, and D.K. Böhme. J. Am. Chem. Soc. **119**, 7055 (1997).
33. J. Wang, G. Javahery, V. Baranov, and D.K. Böhme. Tetrahedron, **52**, 5191 (1996).
34. V. Baranov, J. Wang, A.C. Hopkinson, and D.K. Böhme. J. Am. Chem. Soc. **119**, 2040 (1997).
35. V. Baranov and D.K. Böhme. Int. J. Mass Spectrom. Ion Processes, **149**/**150**, 543 (1995).
36. R.C. Haddon. Science (Washington, D.C.), **261**, 1545 (1993).
37. S. Petrie and D.K. Böhme. Nature (London), **365**, 426 (1993).
38. H. Becker, L.T. Scott, and D.K. Böhme. Int. J. Mass Spectrom. Ion Processes, **167**/**168**, 519 (1997).
39. K. Raghavachari and C.M. Rohlfing. J. Phys. Chem. **95**, 5768 (1991).
40. D. Bakowski and W. Thiel. J. Am. Chem. Soc. **113**, 3704 (1991).
41. J.C. Hanson and C.E. Nordman. Acta Crystallogr. Sect. B: Struct. Crystallogr. Cryst. Chem. **32**, 1147 (1976).
42. J.M. Hawkins, A. Meyer, and M.A.J. Solow. J. Am. Chem. Soc. **115**, 7499 (1994).
43. J. Ahrens, M. Bachmann, Th. Baum, J. Griesheimer, R. Kovacs, P. Weilmünster, and K.-H. Homann. Int. J. Mass Spectrom. Ion Processes, **138**, 133 (1994).
44. S. Petrie, G. Javahery, and D.K. Böhme. Astron. Astrophys. **271**, 662 (1993).
45. S.G. Kukolich and D.R. Huffman. Chem. Phys. Lett. **182**, 263 (1991).
46. H. Thomann, M. Bernardo, and G.P. Miller. J. Am. Chem. Soc. **114**, 6593 (1992).
47. R.D. Bolskar, R.S. Mathur, and C.A. Reed. J. Am. Chem. Soc. **118**, 13093 (1996).